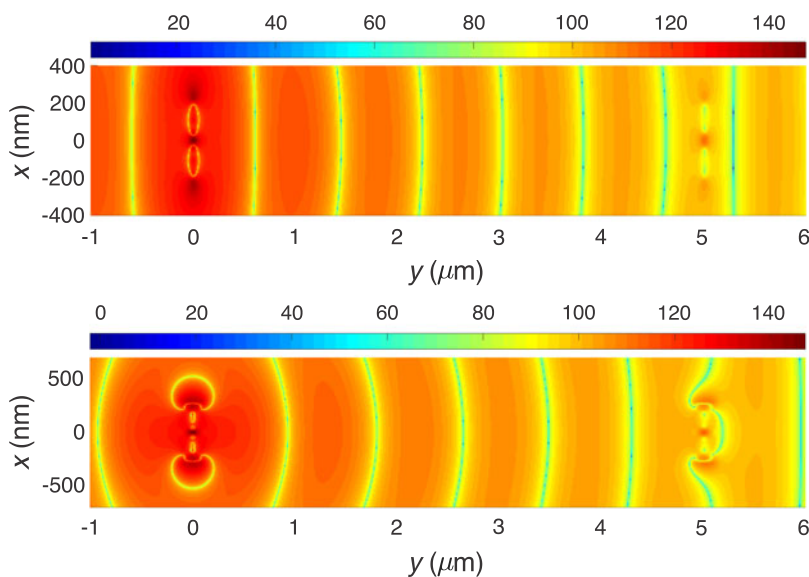


Broadband Wireless Optical Nanolink Composed by Dipole-Loop Nanoantennas

Volume 10, Number 2, April 2018

Janilson Leão de Souza
Karlo Queiroz da Costa



DOI: 10.1109/JPHOT.2018.2810842

1943-0655 © 2018 IEEE

Broadband Wireless Optical Nanolink Composed by Dipole-Loop Nanoantennas

Janilson Leão de Souza ^{1,2} and Karlo Queiroz da Costa¹

¹Department of Electrical Engineering, Federal University of Para, Belém, PA 66075-110, Brazil

²Department of Electrotechnology, Federal Institute of Education, Science and Technology of Para, Tucuruí, PA 68464-000, Brazil

DOI:10.1109/JPHOT.2018.2810842

1943-0655 © 2017 IEEE. Translations and content mining are permitted for academic research only.

Personal use is also permitted, but republication/redistribution requires IEEE permission.

See http://www.ieee.org/publications_standards/publications/rights/index.html for more information.

Manuscript received January 15, 2018; revised February 13, 2018; accepted February 25, 2018. Date of publication March 7, 2018; date of current version March 26, 2018. Corresponding author: Janilson Leão de Souza (e-mail: janilson@ufpa.br).

Abstract: In this paper, a broadband wireless optical nanolink with plasmonic optical nanoantennas is theoretically proposed and analyzed. The nanolink is formed by linear dipole-loop nanoantennas for transmitter and receiver. The analysis is performed using the linear method of moments with equivalent surface impedance, where we apply a voltage source in the transmitting antenna and connect a load in the receiving antenna. The power received in the load is investigated as a function of frequency and distance between transmitter and receiver. In addition, a comparison is made between this wireless nanolink with a bifilar optical transmission line. The results show that the proposed nanolink, with dipole-loop nanoantenna, can increase the operating bandwidth in the range of 179.1–202.5 THz, when compared with conventional nanolink based only on dipole antennas. In addition, wireless nanolinks, based on dipole or dipole-loop antennas, are more suitable than wired nanolink for distances above approximately 22 μm .

Index Terms: Wireless optical nanolink, plasmonic nanoantennas, broadband dipole-loop antennas, method of moments.

1. Introduction

Plasmonic optical nanoantennas are metal devices developed to transmit, receive, amplify and confine optical fields [1]. These devices are analogous to radiofrequency antennas, however, they present significant differences. For example, in the resonant properties, where metallic nanostructures have effective resonant wavelength smaller than the wavelength of incident light [2], which makes possible the confinement of optical fields in small regions beyond the light diffraction limit [3].

These intriguing properties of optical antennas allow the manipulation of light at nanoscale and enable its integration into optical chip applications [4], also opening perspectives for new devices such as integrated wireless detection and communication systems [5]. In addition, these antennas can be applied in photovoltaic devices [6]–[10], amplify fluorescent emission spectroscopy [11], probe for high-resolution optical microscopy [12], amplified Raman scattering (SERS) [13], [14], treatment of cancer in medicine [15], plasmonic laser and optical data storage [16], fiber optics [17], biosensor [18], plasmonic optical circuit [4], [19]–[21], [23] and optical nanolink wireless, that can be used, for example, to interconnect different devices in an integrated nanophotonic circuit [24]–[27].

In this last application, wireless nanolinks, formed by transmitter and receiver nanoantennas have been investigated in literature. In [24], the power transmission of the wireless nanolink, composed

of dipole antennas, is compared to that of a wired nanolink formed by a perfectly matched plasmonic waveguide. In [25], it was shown the signal routing for different receivers when controlling and directing the radiation of the transmitting dipole antenna, in addition it is presented a better result of power transmission using a nanoantenna array. In [26], dipole antennas were used in a nanolink, where it was shown that the proposed system can improve the speed of information transmission when compared to wired nanolink. In [27], horn and dipole antennas in nanolinks were compared, where the horn antenna showed better performance in relation to the dipole antenna, because it presented spectral response in ultrawide bandwidth covering the entire wavelength range of optical telecommunications considered. These studies have in common the analysis of nanolinks using dipole antennas, in addition, one conclusion is that wireless optical nanolinks may have less losses compared to wired link, depending on the distance between the transmitter and receiver antennas, which is important for future integrated plasmonic nanocircuits and nanotelecommunications in general.

In this paper, a broadband wireless optical nanolink, formed by transmitter and receiver nanoantennas, is theoretically proposed and analyzed. The broadband nanoantenna is composed by a combination of loop and dipole antennas. These composite nanoantennas have already been analyzed in isolated situations and connected in OTL [23]. However, the present work investigates for the first time these nanoantennas in wireless nanolinks for broadband operation.

The numerical analysis of the radiation problems considered in this work is done by the linear method of moments (MoM), in the same way that it was done in [22], [23], and [28]. In this analysis, we compare the power transmission, or received power at receiver, in wireless and wired nanolinks. In addition, comparisons of nanolinks based on dipole and dipole-loop antennas are made. The results show that the proposed nanolink, using dipole-loop nanoantennas, can increase the operational bandwidth when compared to nanolink based only in dipole antennas, within the considered optical telecommunications bandwidth. In addition, wireless nanolinks, based on dipole or dipole-loop antennas, present better results from distance approximately above 22 μm in comparison to wired nanolinks.

2. Theory

This section presents a brief description of the geometry and theoretical model of the proposed nanolink. Fig. 1 shows the geometry of the nanolink with dipole-loop nanoantennas, where a voltage source V_S feeds the left nanoantenna, which operates as a transmitter and converts near field into optical radiation propagating in free space. This feeding can be realized, for example, by an optical aperture probe with focused Gaussian beam coupled to transmitting antenna [22]. The nanoantenna located to the right of this figure operates as a receiver, where it captures the outer radiation incoming from the transmitting antenna and converts it to Z_C load as received power. Also, a near-field scanning optical microscopy (NSOM) can be used, for example, to capture the intensity of this received signal and send it to photodetector [26].

The nanolink elements are formed by cylindrical gold conductors and are located in the free space. The transmitter and receiver nanoantennas are formed by the combination of a dipole and a rectangular loop (see Fig. 1) electromagnetically coupled [23]. The dipole of the transmitting antenna has a total length of $2h_{dT} + d_T$, radius a_{dT} , gap d_T of the voltage source, and is located in the plane $z = 0$, positioned along the x axis, and centered at the origin. The dipole of the receiving antenna has total length $2h_{dR} + d_R$, radius a_{dR} , and gap d_R where a load Z_C is connected. This receive dipole is located in the plane $z = 0$, displaced at a distance d_{TR} in relation to the dipole axis of the transmitting antenna. The transmitter loop element has length $H_{eT} + 2a_{eT}$, width $W_{eT} + 2a_{eT}$, radius a_{eT} , and the parameters d_{WT} and d_{HT} are as distances between the surfaces of the dipole and loop elements. The loop of the receiving antenna has length $H_{eR} + 2a_{eR}$, width $W_{eR} + 2a_{eR}$, radius a_{eR} , and the parameters d_{WR} and d_{HR} are the distances between the surfaces of the dipole and loop elements.

This proposed optical wireless nanolink is numerically investigated by the linear MoM, where we used it to solve the integral equation of the electric field, with linear approximation of the

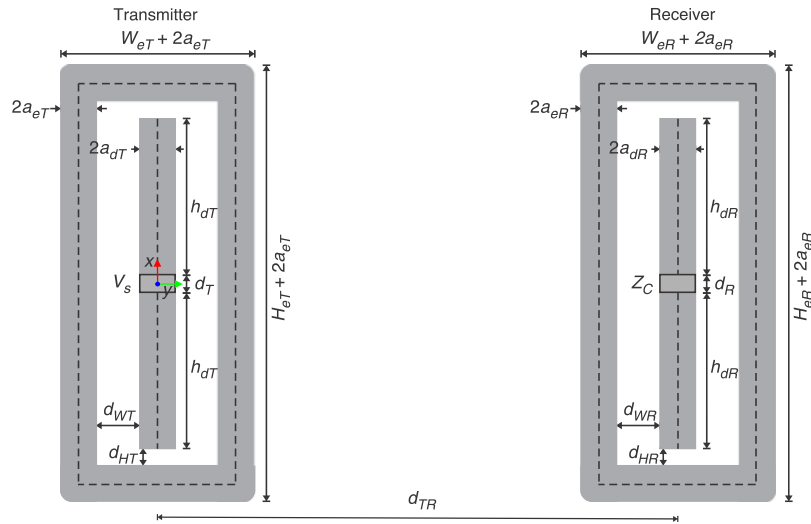


Fig. 1. Geometry of wireless optical nanolink using dipole-loop nanoantennas, transmitter (left) and receiver (right).

longitudinal current, finite surface impedance to represent the losses of the conductors, sinusoidal basis functions, and rectangular pulse for test functions. The dielectric constant of Au is given by the Lorentz-Drude complex permittivity model. A detailed description of this model can be found in [22], [23], and [28].

3. Results

3.1 Transmitting Nanoantenna

In this section, the dipole-loop transmitting antenna of Fig. 1 is analyzed separately. For this analysis, the parameters used are: $h_{dT} = 220$ nm, $a_{dT} = 20$ nm, $d_T = 20$ nm, $d_{WT} = 50$ nm, $d_{HT} = 20$ nm, $a_{eT} = 20$ nm, $W_{eT} = 2a_{eT} + 2a_{dT} + 2d_{WT}$ and $H_{eT} = 2h_{dT} + d_T + 2a_{eT} + 2d_{HT}$. These parameters were used for the isolated antenna, and also for the nanolink, to operate within an optical wavelength band used in telecommunications, where this band varies from the O band (1260 nm or about 238 THz) to the 10 U band (1675 nm or about 179 THz).

Fig. 2 shows the results obtained for the transmitting nanoantenna without the loop [see Fig. 2(a)] and with the loop [see Fig. 2(b)]. In (a) and (b) are shown the input impedance (Z_{in}), electric near-field distribution ($E = 20\log_{10}(|Re(E_x)|)$) in the plane $z = 30$ nm and the 3D far-field gain radiation pattern.

The input impedances are compared with the finite element method (FEM), by using the commercial software Comsol Multiphysics [29]. This simulation in Comsol was done to show the great precision and convergence of MoM. The results of Z_{in} show that the electromagnetic coupling between the dipole and loop modifies the input impedance of the dipole-loop antenna compared to that antenna without loop. In addition, the resonances are shifted to lower frequencies according to the resonant properties of metal nanostructures [2]. We observe a shift of the first resonance from 191.9 THz (dipole) to 185.1 THz (dipole-loop) and the second resonance from 263.8 THz (dipole) to 256.4 THz (dipole-loop).

The near-field and far-field results were calculated at the central frequencies 195 and 171 THz, of the reflection coefficient bandwidth (see Fig. 3), for the transmitting antenna without and with the loop, respectively. In the result of the electric near-field distribution, we observe a more spherical wave front in Fig. 2(b) due the loop, which it possess a geometry more spherical in this plane. The result of the 3D far-field gain radiation pattern shows that the shape of these diagrams

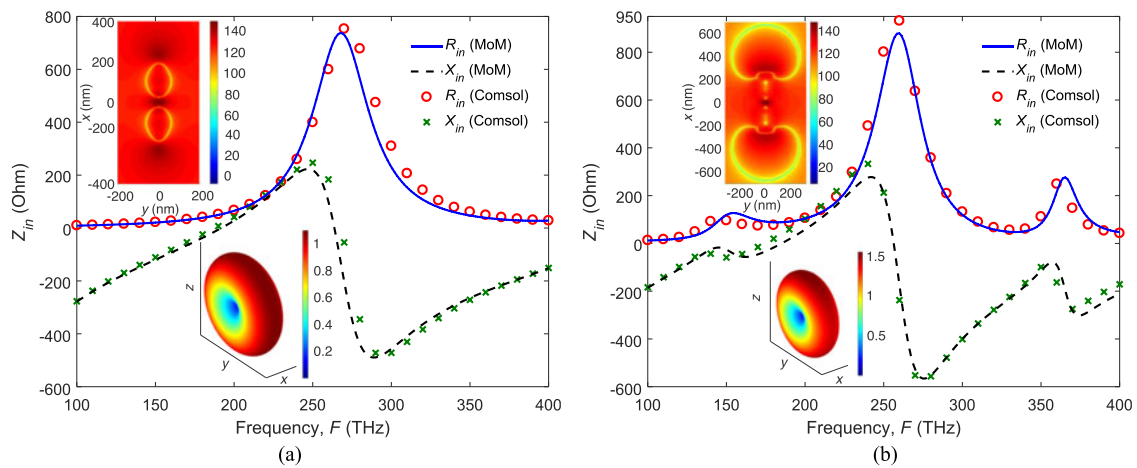


Fig. 2. Results for isolated transmitter antennas: (a) dipole and (b) dipole-loop. (a) Input impedance (Z_{in}) varying with frequency, electric near-field distribution in plane $z = 30$ nm (top left) and 3D far-field gain radiation pattern (low left) both for $F = 195$ THz. (b) Input impedance (Z_{in}) varying with frequency, electric near-field distribution in the plane $z = 30$ nm (top left) and 3D far-field gain radiation pattern (low left) both for $F = 171$ THz.

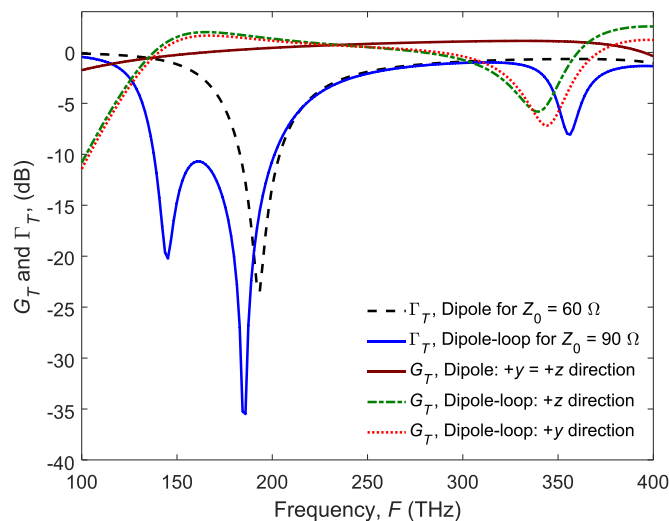


Fig. 3. Gain (G_T), in the $+y$ and $+z$ directions, and reflection coefficient (Γ_T), for $Z_0 = 60 \Omega$ and $Z_0 = 90 \Omega$, of the dipole and dipole-loop transmitting antenna, respectively.

is approximately equal to that of an infinitesimal dipole, which proves that these antennas are electrically small with respect to wavelength. The diagrams present a maximum gain of 1.0954 and 1.5687 for the transmitting antenna without and with the loop, respectively. In addition, the diagram is symmetrical for the case of the dipole antenna and a little asymmetrical for the case of the dipole-loop antenna. This symmetry of the dipole antenna and asymmetry of the dipole-loop antenna is best seen in Fig. 3, where the gain of the transmitting antenna with and without the rectangular loop were calculated in the $+y$ and $+z$ directions.

Fig. 3 shows, in dB, the reflection coefficient and the gain, in the $+y$ and $+z$ directions, of the dipole and dipole-loop transmitting antenna. The reflection coefficient is given by $\Gamma_T = 20\log_{10}|(Z_{in} - Z_0)/(Z_{in} + Z_0)|$, where Z_{in} is the input impedance of the nanoantenna and Z_0 is the characteristic impedance of a given feed transmission line. From the reflection coefficient results, the bandwidth

is calculated by $B = 200 [(F_s - F_i)/(F_s + F_i)]$, where F_s is the upper frequency and F_i the lower frequency for the -10 dB level of the reflection coefficient.

The gain (see Fig. 3) of the dipole-loop antenna has higher values than the gain of the dipole antenna, in both directions, around the resonances of the dipole antennas (near 184 THz of Γ_T of the dipole-loop antenna) and dipole-loop (about 145 THz of Γ_T of the dipole-loop antenna), and at other frequency points. Due the geometry's symmetry, the gain of the dipole antenna is the same in the $+y$ and $+z$ directions. The gain of the dipole-loop antenna is higher in the $+z$ direction than the $+y$ direction, in almost all frequency points. The curves of the reflection coefficient show that the dipole-loop antenna has a broad bandwidth of $B = 37.1\%$ at the level of $\Gamma_T = -10$ dB, considering connection to a line with $Z_0 = 90 \Omega$. The dipole antenna has a narrow bandwidth of $B = 10.1\%$ at the level of $\Gamma_T = -10$ dB, considering connection to a line with $Z_0 = 60 \Omega$.

The bandwidth of the dipole and dipole-loop antennas are centered ($F_c = (F_s + F_i)/2$) at frequencies 195 and 171 THz respectively, which means that these points represent a sample of what occurs around these points within the band. Thus, the transmitting antenna with and without the rectangular loop can be used, in applications, to operate around or at the central frequency of the band. For application in wireless optical nanolink, these transmitting antenna with and without loop can be used because they operates at frequency points within the considered optical telecommunications band.

3.2 Wireless Optical Nanolink

In this section is analyzed the complete nanolink shown in Fig. 1. Two following models of nanolinks will be analyzed: one with only dipole antennas and other with dipole-loop antennas. The parameters used for the transmitting and receiving antennas are the same to those used in Section 3.1 for the transmitting antenna. Also, the values of load impedance Z_C is equal to Z_0 , where for nanolink with dipole antennas $Z_C = 60 \Omega$ and for the nanolink with dipole-loop antennas $Z_C = 90 \Omega$.

For the nanolink case with dipole antennas, it was designed to operate around the central frequency of bandwidth of the dipole's reflection coefficient Γ_T (see Fig. 3). In the case of the nanolink with loop, it was designed to operate above the central frequency of bandwidth of the dipole-loop's reflection coefficient (see Fig. 3). In other words, both nanolinks were designed to operate within the considered optical band.

The spectral response of the nanolinks can be investigated by calculating the power transmission. This power transmission can be calculated approximately by using the analytical Friis transmission equation, as was done in [24] and [27], or more accurately by the MoM numerical model [22], [23], [28]. The definition of this parameter is the ratio between the power delivered to the load Z_C and the power delivered by the voltage source at the input terminals of the transmitting antenna. The model of calculation of transmission power by the MoM model is more advantageous than other methods, for example, the finite difference in time domain (FDTD) and FEM. This is because in these methods it would be computationally impractical due the great distances considered, where it would require a very large amount of memory for the all domain of analysis. On the other hand, the MoM does not have this computational problem because we discretize only the antenna's geometry [23]. For example, in [27], for nanolink analysis in lower distances, the FDTD was used, however, to calculate the power transmission as a function of distance, the authors first calculated the transmitter and receiver antenna gains to be able to apply the Friis transmission equation.

Fig. 4(a) shows the power transmission versus frequency for the nanolinks with the receiving antennas positioned at a distance $d_{TR} = 50 \mu\text{m}$ for all cases. Two cases of dipole-loop nanolinks are shown: parallel loops (loops in the xy plane) and perpendicular loops (loops in the xz plane) in relation to the direction of propagation of the link (direction $+y$). This change of plane of the loop was done with purpose of showing that the transmission improves for some frequency points, since the gain of the transmitting antenna improves in the $+z$ direction (see Fig. 3). This improvement is not only a function of gain of the isolated antenna (see Fig. 3), but it also depends on the impedance matching in the receiver circuit. In Fig. 4(a), the power transmission of the nanolink with dipole antennas shows a wide fluctuation around the central frequency (195 THz), which characterizing a

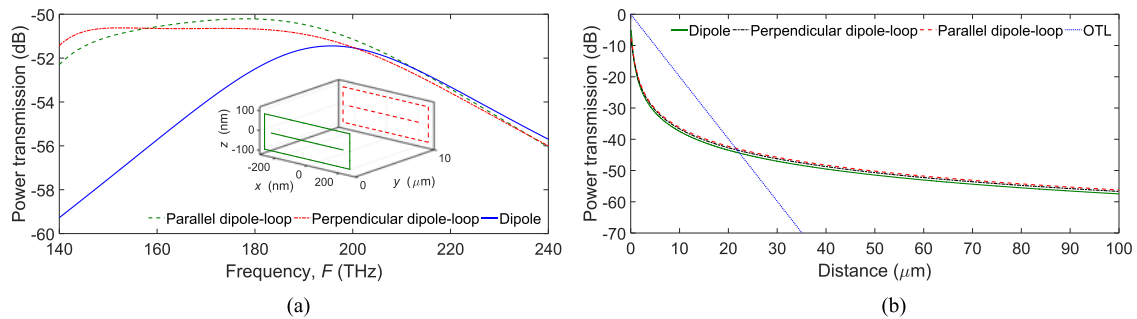


Fig. 4. (a) Power transmission versus frequency for three different nanolinks with $d_{TR} = 50 \mu\text{m}$. Inset is shown the geometry for nanolink with perpendicular loops to the direction of propagation, where the loop is in xz plane. (b) Power transmission versus distance, for $F = 194 \text{ THz}$, in the case of nanolink based on dipole antennas (solid line), $F = 180 \text{ THz}$ for nanolink using dipole-loop antennas (dashed line for parallel loop and dashed-dotted line for perpendicular loop to direction of propagation) and $F = 194 \text{ THz}$ in case of cylindrical OTL (dotted line).

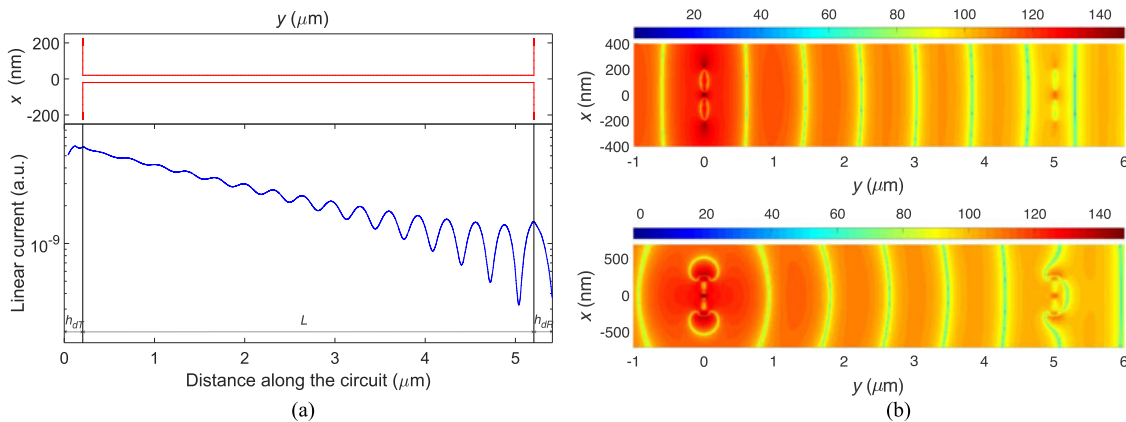


Fig. 5. (a) Top: Geometry of the wired nanolink with OTL in the xy plane, with $h_{dT} = h_{dR} = 220 \text{ nm}$, $a_{dT} = a_{dR} = 20 \text{ nm}$, $L = 5 \mu\text{m}$, low: linear current distribution along the nanocircuit. (b) Electric near-field distribution, $E = 20\log_{10}(|\text{Re}(E_x)|)$, in the plane $z = 30 \text{ nm}$ for the frequencies, 194 THz and 180 THz , respectively, of nanolinks based on dipole antennas (top) and dipole-loop (low), for a distance between transmitting and receiving antennas of $5 \mu\text{m}$.

narrow bandwidth of this nanolink. On the other hand, nanolink with dipole-loop antennas presents an evident characteristic of wide bandwidth, since the power transmission remains approximately constant in the range of 144 to 186 THz . In other words, the nanolink with dipole-loop antennas possesses a broad bandwidth than the conventional nanolink with only dipoles antennas.

Fig. 4(b) shows the behavior of power transmission as a function of distance, for nanolinks based on dipole and dipole-loop antennas (parallel and perpendicular). In addition, the power transmission of a bifilar cylindrical OTL is shown in the figure, where this OTL is connected between the transmitting and receiving antennas of Fig. 1, without the loops, forming an optical nanocircuit [see Fig. 5(a)]. The transmitter antenna is fed by the same Gaussian beam of reference [22], changing only the frequency of the beam to 194 THz . The OTL has a wire radius of $a_L = 15 \text{ nm}$, and the antennas have the same dimensions of the nanolink parameters without the rectangular loop.

The losses in OTL are calculated in the same way as it was done in [22], where the OTL loss constant α is calculated, which is almost constant for the principal mode propagating in the OTL, and can be obtained, approximately, by the average value of the inclination of the current curve versus distance along the length L of the OTL [see Fig. 5(a)]. Thus, $\alpha = \Delta I / \Delta L$, where ΔI is the

average variation of the current amplitude in decibels (dB), over a given distance ΔL in the OTL. The α parameter found for OTL, considering a line with $L = 5 \mu\text{m}$ in length, was approximately 0.0019954 dB/nm.

In Fig. 4(b) it is observed that the nanolink power transmission curve, based on dipole antennas, agrees with the found in the literature [24], [25], [27], for example, this results have smaller path loss (power transmission versus distance) than that of paper [27], at operating frequency of 194 THz. For the case of nanolink using dipole-loop antennas, no studies were found in the literature to compare with the result of Fig. 4(b). For the OTL case, the loss agrees with that found in [24], [25], and [27], presenting similar losses to those works. Fig. 4(b) also shows that wireless optical nanolinks may have smaller losses compared to wired nanolink, starting from a given distance, where for the cases considered in this work this distance is $22 \mu\text{m}$. This shows that optical nanolinks based on antennas are more suitable than OTL for communication at long distances. In addition, the nanolink with dipole-loop antennas presents an improvement of little more than 1 dB, in relation to the nanolink with dipole antennas.

Finally, Fig. 5(b) shows the electric near-field distribution ($E = 20\log_{10}(|\text{Re}(E_x)|)$) of the nanolinks, based on dipole antennas (Fig. 1 without loops) and dipole-loop (Fig. 1 with loops), in the plane $z = 30 \text{ nm}$, for a distance between the transmitting and receiving antennas of $5 \mu\text{m}$. We observed that for the case with dipole-loop [see Fig. 5(b)] the wave front is more spherical due to the presence of the loop, which has components of current in the x and y directions in its conductors, which makes the radiation with a more spherical symmetry around the antenna, at this plane, when compared to the isolated dipole.

4. Conclusion

In this work, an application of cylindrical plasmonic nanoantenna in broadband wireless optical nanolink was theoretically proposed and analyzed. Broadband dipole-loop combination type transmitter and receiver antennas were used. Also for comparison, the conventional link composed only by dipoles antennas was considered. The nanolinks were theoretically analyzed by the linear MoM with surface impedance of the conductors, where some results were obtained by finite element method for comparison. The results show that by using dipole-loop antennas in the nanolink instead of conventional dipoles, it is possible to increase the operating bandwidth of the system to the range of 179.1–202.5 THz [see Fig. 4(a)], which is within the optical telecommunications band considered. In other words, this type of nanolink, with relatively simple geometry, can be used as solution for broadband radio data communication at nanoscale. In addition, the wireless nanolinks based on dipole or dipole-loop antennas presented better transmission, approximately, above the distance of $22 \mu\text{m}$ [see Fig. 4(b)], when compared to the equivalent wired nanolinks with bifilar OTL.

Acknowledgment

The authors would like to thank the Electromagnetic Laboratory (LEMAG) of Federal University of Para, Tucuruí, PA, Brazil, where the principal results were obtained.

References

- [1] L. Novotny and N. V. Hulst, "Antennas for light," *Nature Photon.*, vol. 5, pp. 83–90, 2011.
- [2] L. Novotny, "Effective wavelength scaling for optical antennas," *Phys. Rev. Lett.*, vol. 98, 2007, Art. no. 266802.
- [3] D. K. Gramotnev and S. I. Bozhevolnyi, "Plasmonics beyond the diffraction limit," *Nature Photon.*, vol. 4, pp. 83–91, 2010.
- [4] Q. Gao, S. Liverman, and A. X. Wang, "Design and characterization of high efficiency nanoantenna couplers with plasmonic integrated circuit," *J. Lightw. Technol.*, vol. 35, no. 15, pp. 3182–3188, Aug. 2017.
- [5] P. Russer, N. Fichtner, P. Lugli, W. Porod, J. A. Russer, and H. Yordanov, "Nanoelectronics-based integrate antennas," *IEEE Microw. Mag.*, vol. 11, no. 7, pp. 58–71, Dec. 2010.
- [6] N. F. F. Areed, S. M. El Malt, and S. S. A. Obayya, "Broadband omnidirectional nearly perfect plasmonic absorber for solar energy harvesting," *IEEE Photon. J.*, vol. 8, no. 5, Oct. 2016, Art. no. 4802718.

- [7] F. Taghian, V. Ahmadi, and L. Yousefi, "Enhanced thin solar cells using optical nano-antenna induced hybrid plasmonic travelling-wave," *J. Lightw. Technol.*, vol. 34, no. 4, pp. 1267–1273, Feb. 2016.
- [8] A. M. A. Sabaawi, C. C. Tsimenidis, and B. S. Sharif, "Analysis and modeling of infrared solar rectennas," *IEEE J. Sel. Topics Quantum Electron.*, vol. 19, no. 3, May/Jun. 2013, Art. no. 9000208.
- [9] K. Q. Le, "Broadband light trapping in thin organic photovoltaic cells using plasmonic resonant antennas," *J. Appl. Phys.*, vol. 114, 2013, Art. no. 084504.
- [10] H. A. Atwater and A. Polman, "Plasmonics for improved photovoltaic devices," *Nature Mater.*, vol. 9, pp. 205–213, 2010.
- [11] R. M. Bakker, H.-K. Yuan, Z. Liu, V. P. Drachev, A. V. Kildishev, and V. M. Shalaev, "Enhanced localized fluorescence in plasmonic nanoantennae," *Appl. Phys. Lett.*, vol. 92, 2008, Art. no. 043101.
- [12] T. H. Taminiau, F. B. Segerink, and N. F. van Hulst, "A monopole antenna at optical frequencies: Single-molecule near-field measurements," *IEEE Trans. Antennas Propag.*, vol. 55, no. 11, pp. 3010–3017, Nov. 2007.
- [13] K. Li, L. Clime, B. Cui, and T. Veres, "Surface enhanced Raman scattering on long-range ordered noble-metal nanocrescent arrays," *Nanotechnology*, vol. 19, 2008, Art. no. 145305.
- [14] K. B. Crozier, W. Zhu, D. Wang, S. Lin, M. D. Best, and J. P. Camden, "Plasmonics for surface enhanced Raman scattering: Nanoantennas for single molecules," *IEEE J. Sel. Topics Quantum Electron.*, vol. 20, no. 3, pp. 152–162, May/Jun. 2014.
- [15] D. DasGupta, G. V. Maltzahn, S. Ghosh, S. N. Bhatia, S. K. Das, and S. Chakraborty, "Probing nanoantenna-directed photothermal destruction of tumors using noninvasive laser irradiation," *Appl. Phys. Lett.*, vol. 95, 2009, Art. no. 233701.
- [16] E. Cubukcu, N. Yu, E. J. Smythe, L. Diehl, K. B. Crozier, and F. Capasso, "Plasmonic laser antennas and related devices," *IEEE J. Sel. Topics Quantum Electron.*, vol. 14, no. 6, pp. 1448–1461, Nov./Dec. 2008.
- [17] Q. Gao, F. Ren, and A. X. Wang, "Direct and efficient optical coupling into plasmonic integrated circuits from optical fibers," *IEEE Photon. Technol. Lett.*, vol. 28, no. 11, pp. 1165–1168, Jun. 2016.
- [18] M. Alavirad, L. Roy, and P. Berini, "Optimization of plasmonic nanodipole antenna arrays for sensing applications," *IEEE J. Sel. Topics Quantum Electron.*, vol. 20, no. 3, May/Jun. 2014, Art. no. 4600308.
- [19] J. Wen, S. Romanov, and U. Peschel, "Excitation of plasmonic gap waveguides by nanoantennas," *Opt. Exp.*, vol. 17, pp. 5925–5932, 2009.
- [20] J.-S. Huang, T. Feichtner, P. Biagioni, and B. Hecht, "Impedance matching and emission properties of nanoantennas in an optical nanocircuit," *Nano Lett.*, vol. 9, pp. 1897–1902, 2009.
- [21] A. Kriesch, S. P. Burgos, D. Ploss, H. Pfeifer, H. A. Atwater, and U. Peschel, "Functional plasmonic nanocircuits with low insertion and propagation losses," *Nano Lett.*, vol. 13, pp. 4539–4545, 2013.
- [22] K. Q. da Costa, V. Dmitriev, J. L. de Souza, and G. Silvano, "Analysis of nanodipoles in optical nanocircuits fed by Gaussian beam," *Int. J. Antennas Propag.*, vol. 2014, 2014, Art. no. 429425.
- [23] J. L. de Souza, K. Q. da Costa, V. Dmitriev, and F. Bamberg, "Broadband dipole-loop combined nanoantenna fed by two-wire optical transmission line," *Int. J. Antennas Propag.*, vol. 2017, 2017, Art. no. 4903747.
- [24] A. Alù and N. Engheta, "Wireless at the nanoscale: Optical interconnects using matched nanoantennas," *Phys. Rev. Lett.*, vol. 104, 2010, Art. no. 213902.
- [25] D. Dregely, K. Lindfors, M. Lippitz, N. Engheta, M. Totzeck, and H. Giessen, "Imaging and steering an optical wireless nanoantenna link," *Nature Commun.*, vol. 5, 2014, Art. no. 5354.
- [26] J. M. Merlo *et al.*, "Wireless communication system via nanoscale plasmonic antennas," *Sci. Rep.*, vol. 6, 2016, Art. no. 31710.
- [27] Y. Yang, Q. Li, and M. Qiu, "Broadband nanophotonic wireless links and networks using on-chip integrated plasmonic antennas," *Sci. Rep.*, vol. 6, 2016, Art. no. 19490.
- [28] K. Q. da Costa and V. Dmitriev, "Simple and efficient computational method to analyze cylindrical plasmonic nanoantennas," *Int. J. Antennas Propag.*, vol. 2014, 2014, Art. no. 675036.
- [29] *COMSOL Multiphysics 5.2*, COMSOL, Inc., Los Angeles, CA, USA. 2015. [Online]. Available: <http://www.comsol.com>